

An accurate analytic description of neutrino oscillations in matter

E. Kh. Akhmedov^{a,b*} and Viviana Niro^{a†}

^a*Max-Planck-Institut für Kernphysik, Postfach 103980
D-69029 Heidelberg, Germany*

^b*National Research Centre Kurchatov Institute
Moscow, Russia*

October 29, 2018

Abstract

A simple closed-form analytic expression for the probability of two-flavour neutrino oscillations in a matter with an arbitrary density profile is derived. Our formula is based on a perturbative expansion and allows an easy calculation of higher order corrections. The expansion parameter is small when the density changes relatively slowly along the neutrino path and/or neutrino energy is not very close to the Mikheyev-Smirnov-Wolfenstein (MSW) resonance energy. Our approximation is not equivalent to the adiabatic approximation and actually goes beyond it. We demonstrate the validity of our results using a few model density profiles, including the PREM density profile of the Earth. It is shown that by combining the results obtained from the expansions valid below and above the MSW resonance one can obtain a very good description of neutrino oscillations in matter in the entire energy range, including the resonance region.

*email: akhmedov@mpi-hd.mpg.de

†email: viviana.niro@mpi-hd.mpg.de

1 Introduction

In most neutrino oscillation experiments neutrinos propagate substantial distances in matter before reaching a detector, and therefore an accurate description of neutrino oscillations in matter [1, 2] is an important ingredient of the analyses of the data. For a matter of an arbitrary density profile the neutrino evolution equation admits no closed-form solution, and one usually has to resort to numerical methods. While numerical integration of the evolution equation usually poses no problem, it is still highly desirable to have approximate analytic solutions, which may provide a significant insight into the physics of neutrino oscillations in matter, clarify the dependence of the oscillation probabilities on the neutrino parameters and in many cases help save the CPU time. To this end, a number of analytic solutions of the neutrino evolution equation in matter, based on various approximations, has been developed (for recent studies, see e.g. [3, 4, 5, 6, 7, 8, 9, 10]).

In this paper we derive a simple analytic expression for the two-flavour oscillation probability valid for an arbitrary matter density profile. We employ a perturbative approach based on the expansion in a parameter which is small when the density changes relatively slowly along the neutrino path and/or neutrino energy is not very close to the Mikheyev-Smirnov-Wolfenstein (MSW) [1, 2] resonance energy. Our approximation is not equivalent to the adiabatic approximation and actually goes beyond it. We demonstrate the validity of our results using a few model density profiles, including the important PREM profile [11], which gives a realistic description of matter density distribution inside the Earth. We also show that, by combining the results obtained for the energies below and above the MSW resonance ones, one can obtain an excellent description of neutrino oscillations in matter in the entire energy range. The simple form of our result and the wide range of its applicability are the two main advantages of this approach.

An approach similar to ours has been employed in [12, 7]. Unlike in those publications, in the present work we do not confine ourselves to the leading approximation, but also calculate the first and second order corrections and show that this improves the accuracy of the approximation drastically.

The paper is organized as follows. In Sec. 2 we present the formalism used to derive our analytic solution. In Sec. 3 we apply this method to the case of a parabolic and a power law matter potentials. In Sec. 4 we present the results obtained in the case of the realistic PREM Earth's density profile. We discuss our results and conclude in Sec. 5.

2 The formalism

In a number of important cases the full three-flavour neutrino oscillations can to a very good accuracy be reduced to effective two-flavour ones. These include $\nu_e \leftrightarrow \nu_\mu(\nu_\tau)$ oscillations either in the limit of vanishingly small 1-3 mixing, when the oscillations are essentially driven by the “solar” parameters Δm_{21}^2 and θ_{12} , or at sufficiently high energies ($E \gtrsim 1$ GeV for oscillations in the Earth), when the 1-2 mixing in matter is strongly suppressed; in that case the oscillation probabilities are essentially independent of the “solar”

parameters and are governed by Δm_{31}^2 and θ_{13} . For definiteness, in our numerical examples we will concentrate on the second case, though our general discussion will be valid in both situations.

Two-flavour oscillations of neutrinos in matter are described by the Schrödinger-like evolution equation [1, 2]

$$i \begin{pmatrix} \dot{\xi} \\ \dot{\eta} \end{pmatrix} = \begin{pmatrix} -A & B \\ B & A \end{pmatrix} \begin{pmatrix} \xi \\ \eta \end{pmatrix}, \quad (1)$$

where the overdot denotes the differentiation with respect to the coordinate, and ξ and η are respectively the probability amplitudes to find ν_e and ν_a , the latter being a linear combination of ν_μ and ν_τ . In the limit when the 1-3 mixing vanishes, $\theta_{13} \rightarrow 0$, one has $\nu_a = \cos \theta_{23} \nu_\mu - \sin \theta_{23} \nu_\tau$, whereas in the situations when the solar parameters play practically no role (e.g. for oscillations of high-energy neutrinos in the Earth), $\nu_a = \sin \theta_{23} \nu_\mu + \cos \theta_{23} \nu_\tau$. The quantities A and B in Eq. (1) are

$$\begin{aligned} B &= \delta \sin 2\theta_0, \\ A(x) &= \delta \cos 2\theta_0 - V(x)/2. \end{aligned} \quad (2)$$

Here the function $A(x)$ depends on the electron number density $N_e(x)$ through the Wolfenstein potential $V(x)$ defined as

$$V(x) = \sqrt{2} G_F N_e(x) \cong 7.54 \times 10^{-14} Y_e(x) \rho(x) (\text{g/cm}^3) \text{ eV},$$

where G_F is the Fermi constant, $\rho(x)$ is the mass density of matter and $Y_e(x)$ is the number of electrons per nucleon. The parameter δ is defined as $\delta \equiv \Delta m^2/4E$, and θ_0 is the relevant mixing angle in vacuum. In the limit $\theta_{13} \rightarrow 0$ one has $\Delta m^2 = \Delta m_{21}^2$, $\theta_0 = \theta_{12}$, and the $\nu_e \leftrightarrow \nu_\mu(\nu_\tau)$ oscillation probabilities are given by

$$P(\nu_e \rightarrow \nu_\mu; x) = P(\nu_\mu \rightarrow \nu_e; x) = \cos^2 \theta_{23} P_2(x), \quad (3)$$

$$P(\nu_e \rightarrow \nu_\tau; x) = P(\nu_\tau \rightarrow \nu_e; x) = \sin^2 \theta_{23} P_2(x). \quad (4)$$

Here $P_2(x)$ is the effective two-flavour oscillation probability:

$$P_2(x) = P(\nu_e \rightarrow \nu_a; x) \equiv |\eta(x)|^2 \quad (5)$$

(we assume the initial conditions $\xi(0) = 1$, $\eta(0) = 0$). For oscillations of high-energy neutrinos in the Earth one has $\Delta m^2 = \Delta m_{31}^2$, $\theta_0 = \theta_{13}$, and the $\nu_e \leftrightarrow \nu_\mu(\nu_\tau)$ oscillation probabilities are

$$P(\nu_e \rightarrow \nu_\mu; x) = P(\nu_\mu \rightarrow \nu_e; x) = \sin^2 \theta_{23} P_2(x), \quad (6)$$

$$P(\nu_e \rightarrow \nu_\tau; x) = P(\nu_\tau \rightarrow \nu_e; x) = \cos^2 \theta_{23} P_2(x), \quad (7)$$

where, as before, $P_2(x)$ is given by Eq. (5).

Differentiating Eq. (1), one can find decoupled second order differential equations for $\xi(x)$ and $\eta(x)$ [13, 14]. The equation for the transition amplitude $\eta(x)$ reads

$$\ddot{\eta} + (\omega^2 + i\dot{A})\eta = 0, \quad (8)$$

where we have defined the function $\omega(x)$ as

$$\omega^2(x) = A^2(x) + B^2. \quad (9)$$

Note that the instantaneous eigenvalues of the effective Hamiltonian in Eq. (1) are $\pm\omega(x)$. The equation for $\xi(x)$ differs from Eq. (8) by the sign of the \dot{A} term.

It will be convenient for our purposes to rewrite Eq. (8) in the following form:

$$\ddot{\eta} + (\omega^2 - i\dot{\omega})\eta = (-i\dot{\Delta})\eta, \quad (10)$$

where we have introduced the notation

$$\dot{\Delta} \equiv \dot{A} + \dot{\omega}. \quad (11)$$

Eq. (10) cannot in general be solved exactly, but, as we shall see, it admits a simple perturbative solution. To show that, let us first notice that, for energies (or densities) above the MSW resonance one, the quantity $\dot{\Delta}$ on the right hand side of Eq. (10) is small. Indeed, from Eqs. (9) and (2) it follows that for $V/2 - \cos 2\theta_0 \delta \gg \sin 2\theta_0 \delta$ (i.e. for $-A \gg B$) one has $\dot{\omega} \simeq -\dot{A}$, so that $\dot{\Delta} \simeq 0$. The smallness of the parameter $\dot{\Delta}$ allows one to solve Eq. (10) perturbatively, order by order. Expanding in powers of $\dot{\Delta}$, we find the equation for the n th order transition amplitude η_n (with $n > 0$):

$$\ddot{\eta}_n + (\omega^2 - i\dot{\omega})\eta_n = (-i\dot{\Delta})\eta_{n-1}. \quad (12)$$

The zero order transition amplitude η_0 satisfies the equation with the vanishing right hand side:

$$\ddot{\eta}_0 + (\omega^2 - i\dot{\omega})\eta_0 = 0. \quad (13)$$

Its solution for an arbitrary functional dependence of $\omega(x)$ on the coordinate can be readily found by considering the quantity $X_0 \equiv \dot{\eta}_0 - i\omega\eta_0$, which, as follows from (13), satisfies the first-order equation $\dot{X}_0 + i\omega X_0 = 0$. Taking into account that the initial conditions $\xi(0) = 1$, $\eta(0) = 0$ also imply, through Eq. (1), $\dot{\eta}(0) = -iB$, one finds

$$\eta_0(x) = -iB e^{i\phi(x)} \int_0^x dx_1 e^{-2i\phi(x_1)}, \quad (14)$$

where

$$\phi(x) \equiv \int_0^x \omega(x') dx'. \quad (15)$$

This yields the zero-order solution for the two-flavour transition probability $P_2(x)$ [12, 7]:

$$[P_2(x)]_0 \equiv |\eta_0(x)|^2 = B^2 \left| \int_0^x dx_1 e^{-2i\phi(x_1)} \right|^2. \quad (16)$$

Assuming that the amplitude $\eta_{n-1}(x)$ on the right hand side of Eq. (12) is known, one can solve it for η_n . To this end, we introduce the quantity

$$X_n = \dot{\eta}_n - i\omega\eta_n, \quad (17)$$

in terms of which Eq. (12) can be rewritten as

$$\dot{X}_n + i\omega X_n = (-i\dot{\Delta})\eta_{n-1}. \quad (18)$$

This can now be solved by the standard methods. First, we find the general solution of the homogeneous equation

$$\dot{X}_n + i\omega X_n = 0, \quad (19)$$

which gives

$$X_n(x) = F e^{-i\phi(x)} \quad (20)$$

with F an integration constant. Next, the solution of the inhomogenous equation (18) is found by allowing F to depend on the coordinate x and substituting Eq. (20) back into Eq. (18). Taking into account the initial condition $F(0) = \dot{\eta}(0) - i\omega(0)\eta(0) = -iB$, one finds

$$F(x) = \int_0^x dx_1 e^{i\phi(x_1)} \left(-i\dot{\Delta}(x_1) \right) \eta_{n-1}(x_1) - iB. \quad (21)$$

The solution for X_n is now given by Eq. (20) with F replaced by $F(x)$ from Eq. (21). Once X_n is known, it is straightforward to solve Eq. (17) for η_n . This yields

$$\eta_n(x) = e^{i\phi(x)} \int_0^x dx_1 e^{-2i\phi(x_1)} \int_0^{x_1} dx_2 e^{i\phi(x_2)} \left(-i\dot{\Delta}(x_2) \right) \eta_{n-1}(x_2) + \eta_0(x), \quad (22)$$

where we have used Eq. (14). The corresponding n th order effective two-flavour oscillation probability is then found as $[P_2(x)]_n = |\eta_n(x)|^2$.

Eq. (22) represents the main result of our paper. It gives an analytic expression for the oscillation amplitude in the n th order in perturbation theory in terms of the lower-order solutions η_{n-1} and η_0 . For our numerical illustrations we will consider the solutions with $n = 0, 1$ and 2 .

Eq. (22) has been derived under the assumption that $\dot{\Delta}$ is a small parameter. As we pointed out before, this is true for energies above the MSW resonance one. This means that the perturbative approach considered above should, in general, fail for energies below the MSW resonance one. However, a simple modification of the above procedure leads to a description of neutrino oscillations valid below the MSW resonance. In order to show this, let us, instead of casting Eq. (8) in the form (10), rewrite it as

$$\ddot{\eta} + (\omega^2 + i\dot{\omega})\eta = (-i\dot{\Delta})\eta, \quad (23)$$

where $\dot{\Delta}$ is now defined as

$$\dot{\Delta} = \dot{A} - \dot{\omega}. \quad (24)$$

For small vacuum mixing angles, this is a small parameter below the MSW resonance, since in that case $A \gg B$ and so $\dot{\omega} \simeq \dot{A}$. Therefore, we can proceed with the perturbative approach, as before. Comparing Eqs. (23) and (24) with Eqs. (10) and (11) respectively, we see that the two pairs of equations differ only by the sign of $\omega(x)$. Therefore the solution of Eq. (23) can be obtained from Eq. (22) by simply replacing $\omega(x)$ by $-\omega(x)$. This will also change the values of the oscillation probabilities obtained in all orders in perturbation theory except for the zero-order probability which, as can be seen from (16), is invariant with respect to the flip of the sign of $\omega(x)$. As we shall see, by combining the results valid above and below the MSW resonance one can obtain a very good description of neutrino oscillations in matter in the entire energy range.

Let us now discuss the expansion parameter of our perturbative approach. We have found that the corrections to the zero order amplitude η_0 are proportional to $\dot{\Delta} = \dot{A} \pm \dot{\omega}$, where the upper and lower signs refer to the energies above and below the MSW resonance, respectively. These quantities can be expressed through the mixing angle in matter θ_m :¹

$$\dot{\Delta} = \dot{A} \pm \dot{\omega} = -\frac{\dot{V}}{2} [1 \pm \cos 2\theta_m] . \quad (25)$$

Far above the MSW resonance one has $\cos 2\theta_m \simeq -1$, whereas far below the resonance $\cos 2\theta_m \simeq \cos 2\theta_0$, which is close to 1 in the case of small vacuum mixing. This demonstrates the smallness of $\dot{\Delta}$ in its corresponding domains of validity. At the MSW resonance one has $\cos 2\theta_m = 0$, and $\dot{\Delta}$ is only small if \dot{V} is.

An examination of Eq. (22) shows that the expansion parameter of our perturbative approach is actually $\sim |\dot{\Delta}|/\omega^2$ (see Eq. (15)). In various energy domains we have

$$\frac{|\dot{\Delta}|}{\omega^2} = \begin{cases} \frac{|\dot{A}-\dot{\omega}|}{\omega^2} \simeq \frac{|\dot{V}|}{2} \frac{s_2^2 \delta^2}{(c_2 \delta - V/2)^4} & \text{if } (c_2 \delta - V/2) \gg s_2 \delta \quad (\text{below the resonance}) \\ \frac{|\dot{A} \pm \dot{\omega}|}{\omega^2} \simeq \frac{|\dot{V}|}{2 s_2^2 \delta^2} & \text{if } |c_2 \delta - V/2| \ll s_2 \delta \quad (\text{near the resonance}) \\ \frac{|\dot{A}+\dot{\omega}|}{\omega^2} \simeq \frac{|\dot{V}|}{2} \frac{s_2^2 \delta^2}{(V/2 - c_2 \delta)^4} & \text{if } (V/2 - c_2 \delta) \gg s_2 \delta \quad (\text{above the resonance}) \end{cases} \quad (26)$$

where we have used the shorthand notation $c_2 \equiv \cos 2\theta_0$, $s_2 \equiv \sin 2\theta_0$. From Eq. (26) it is easy to see that outside the MSW resonance region the expansion parameter approximately satisfies

$$\frac{|\dot{\Delta}|}{\omega^2} \simeq \sin^2 2\theta_m \frac{|\dot{V}|}{4\omega^2} = \sin 2\theta_m \gamma_{\text{MSW}}^{-1} , \quad (27)$$

where $\gamma_{\text{MSW}} = 4\omega^3/(|\dot{V}|B) = 4\omega^2/(|\dot{V}| \sin 2\theta_m)$ is the MSW adiabaticity parameter. Thus, for small mixing in matter ($\sin 2\theta_m \ll 1$) our approximation is better than the adiabatic one. Close to the resonance the two approaches have comparable accuracy.

¹Note that $\sin 2\theta_m = B/\omega$, $\cos 2\theta_m = A/\omega$.

3 Two examples: parabolic and power law profiles

As a first study, we apply our formalism to two simple density distributions: a parabolic and a power law profile.

For the parabolic profile, we consider the following density distribution:

$$\rho(x) = \rho_0 \left[-k \frac{(x - L/2)^2}{L^2/4} + 1 \right] \quad (28)$$

with

$$\rho_0 = \rho_{max} = 8 \text{ g/cm}^3, \quad k = 1 - \frac{\rho_{min}}{\rho_{max}} = 0.5, \quad (29)$$

and we take the baseline to be $L = 10000$ km. Note that the parabolic density profile represents a good approximation for the density distribution felt by neutrinos in the Earth when they cross only the Earth's mantle.

Next, we analyze the case of the following power-law density distribution:

$$\rho(x) = \rho_0 \left(\frac{x_0}{x_0 + x} \right)^3 \quad (30)$$

with

$$x_0 = 10^3 \text{ km} \quad \text{and} \quad \rho_0 = 10^3 \text{ g/cm}^3, \quad (31)$$

and we consider neutrino propagation over the distance $L = 100$ km. The profile $\rho \propto x^{-3}$ represents a realistic description of the density distribution inside supernovae; note, however, that neutrino flavour transitions in supernovae are more adequately described by different methods (see, e.g., [15]), and so we consider the profile (30) just for illustration.

The results based on our perturbative analytic approach for the profiles (28) and (30) are presented in Fig. 1, where they are compared with the exact ones, obtained by direct numerical integration of the neutrino evolution equation (1). The upper panels show the oscillation probabilities for the parabolic density profile and the lower ones, for the power-law profile (30). The left panels correspond to the expansion valid for energies below the MSW resonance ones, whereas the right panels were obtained for the expansion valid above the resonance energies. As expected, the zero-order approximation gives a good accuracy only outside the MSW resonance region (i.e., outside the intervals $E \sim 3 - 6$ GeV for the parabolic profile and $E \sim 30 - 50$ MeV for the power-law one).² The first-order perturbative results obtained using the expansion valid below the MSW resonance extend slightly the region of good accuracy towards higher energies, closer to the MSW resonance, though in general fail for energies above the MSW resonance, whereas the first-order results found from the expansion valid above the MSW resonance extend the region of good accuracy to lower energies, but in general fail below the MSW resonance. Thus, the first-order calculation taken in their respective domains of applicability allow to achieve

²Note that, since the profiles (28) and (30) (as well as the PREM profile considered in the next section) span a range of matter densities, neutrinos in an interval of energies experience the MSW resonance.

a good description of the exact results closer to the resonance energy than the zero-order solutions do, i.e. they reduce the energy domain in which the approximation fails. At the same time, as can be seen from Fig. 1, the second-order probabilities $|\eta_2|^2$ practically coincide with the corresponding exact results, irrespectively of whether they are obtained using the expansion valid below or above the MSW resonance.

4 Propagation inside the Earth: PREM profile

Neutrinos coming from various sources can propagate inside the Earth before reaching a detector. Examples are atmospheric neutrinos, neutrinos coming from WIMP annihilation inside the Earth or the Sun, as well as neutrinos studied in long-baseline accelerator experiments. We will consider here oscillations of high-energy neutrinos in the Earth, for which we take the matter density distribution as described by the PREM profile [11] (Fig. 3). Note that the PREM profile is symmetric with respect to the midpoint of the neutrino trajectory, and therefore the two-flavour transition amplitude $\eta(x)$ obtained as a solution of Eq. (1) is pure imaginary due to the time reversal symmetry of the problem [16].

In Fig. 2 we present the oscillation probability P_2 as a function of neutrino energy E for two values of the zenith angle of the neutrino trajectory: $\cos\theta_z = -1$, when the neutrinos propagate the longest distance inside the Earth, traversing it along its diameter, and $\cos\theta_z = -0.95$, when they do not cross the inner core of the Earth. As in Fig. 1, we compare the approximate solutions, up to the second order ($[P_2]_2 = |\eta_2|^2$), with the exact solutions found by direct numerical integration of the neutrino evolution equation. In this figure (as well as in Figs. 4 – 6 below) in the left panels we present the oscillation probabilities obtained with the expansion valid below the MSW resonance energy, whereas the right panels show the results found from the expansion valid above the MSW resonance.

It can be seen from Fig. 2 that the zero order probability $|\eta_0|^2$ reproduces accurately the exact one, $|\eta|^2$, only for energies that are outside the resonance region. Indeed, the two solutions nearly coincide for $E \leq 2.5$ GeV and for $E > 7$ GeV, but deviate substantially between these energies. As can be seen from the figure, the accuracy of the first order solutions is slightly better in their respective domain of validity: the solutions $|\eta_1|^2$ valid below the resonance (left panels of the figure) allow an accurate description of the probability for slightly higher energies than $|\eta_0|^2$ does, allowing to come closer to the MSW resonance from below; however, they fail badly (not even being bounded by 1) above the resonance. Likewise, the solutions $|\eta_1|^2$ valid above the resonance (right panels) allow to come closer to the MSW resonance from above, but fail below the resonance.

At the same time, the second-order solution $|\eta_2|^2$ gives quite a good approximation to the exact probability $|\eta|^2$ for all energies, though the solutions obtained through the expansions in their corresponding domains of validity give a better accuracy in these energy domains. By combining the second-order solutions valid below and above the MSW resonance, one can obtain a very good description of the exact oscillation probability practically at all energies, including the resonance region. We have also checked that for trajectories that do not cross the core of the Earth ($\cos\theta_z > -0.838$), for which the matter density pro-

file seen by the neutrinos is relatively smooth, the second order solutions obtained through both expansions essentially coincide with the exact one for all energies.

In Fig. 4 we present the oscillation probability P_2 , obtained in different orders in perturbation theory, as a function of the distance travelled by neutrinos inside the Earth for vertically up-going neutrinos ($\cos \theta_z = -1$) and two values of neutrino energy, $E = 2.8$ GeV and 6 GeV. The figure clearly demonstrates how the accuracy improves with increasing order in perturbation theory; the second order solutions $|\eta_2|^2$ nearly coincide with the exact probability $|\eta|^2$ along the entire neutrino path.

Fig. 5 illustrates the dependence of the analytic solutions on the zenith angle for two values of the neutrino energy, $E = 2.5$ GeV and 6 GeV. For both energies we show the solutions obtained using the expansions valid below and above the MSW resonance. The results agree with our expectations: the second order solution based on the expansion valid below the resonance reproduces the exact one extremely well for $E = 2.5$ GeV but does not give a good accuracy (especially in the core region) for $E = 6$ GeV, while the situation is opposite in the case of the solution corresponding to the expansion valid above the resonance.

Finally, in Fig. 6 we show the dependence of the accuracy of the analytic solutions on the value of the vacuum mixing angle $\theta_0 = \theta_{13}$. As one can see by comparing the upper panels with the corresponding lower ones, with decreasing value of θ_{13} the accuracy of our perturbative expansion improves. This is the consequence of the fact that the expansion parameter (27) decreases with decreasing θ_{13} .

5 Discussion and conclusions

We have developed a perturbative approach for two-flavour neutrino oscillations in matter with an arbitrary density profile. The zero-order oscillation amplitude η_0 satisfies the equation which can be solved analytically for an arbitrary dependence of the matter density distribution on the coordinate along the neutrino path; higher order amplitudes are then obtained from the lower-order ones through a simple perturbative procedure. We have studied the zeroth, first and second order solutions and compared them with each other and with the exact oscillation probability obtained by numerical integration of the neutrino evolution equation. In all orders except the zeroth one, the expansion scheme depends on whether the neutrino energy is above or below the MSW resonance energy, and one has to consider these two cases separately.

While the zero-order result gives a very good accuracy outside the resonance region, higher order corrections are necessary to achieve an accurate description of the oscillation probability in the vicinity of the MSW resonance. We have demonstrated how these corrections, when taken in their respective energy domains of validity, improve drastically the precision of the approximation.

For the smooth density profiles that we have studied, we found that the second order oscillation probability reproduces the exact one extremely well in the whole interval of energies, including the MSW resonance region, independently of whether the expansion

scheme valid below or above the resonance was used. The same is also true for the PREM density profiles in the case when neutrinos cross only the mantle of the Earth, since the density jumps experienced by neutrinos in that case are relatively small. The high accuracy of the second order approximation for smooth density profiles is related to the fact that our expansion parameter, Eq. (27), is proportional to $|\dot{V}|$. This parameter is smaller than the expansion parameter of the adiabatic approximation by the factor $\sin 2\theta_m$ and therefore our approach gives a better accuracy than the adiabatic expansion when the mixing in matter is small. Note that a different expansion of the same evolution equation (8) was employed in [17].

For energies above the MSW resonance, our expansion parameter is essentially

$$\frac{|\dot{\Delta}|}{\omega^2} \simeq \sin^2 2\theta_m \frac{|\dot{V}|}{V^2}. \quad (32)$$

For the PREM density profile of the Earth, the function $|\dot{V}|/V^2$ is plotted in the right panel of Fig. 3. As can be seen from the figure, in most of the coordinate space the value of this function does not exceed 0.25. The spikes corresponding to the density jumps, though quite high, are very narrow; they do not destroy our approximation because their contributions get suppressed due to the integrations involved in the calculation of the higher-order corrections to the oscillation amplitude (see Eq. (22)). Still, these contributions are not negligible, especially for neutrinos crossing the Earth's core. As a result, for core-crossing neutrinos with energies close to the MSW resonance ones, even the second-order oscillation probabilities are only adequate when taken in their respective energy domains of validity. By combining the solutions valid below and above the MSW resonance one obtains a very accurate description of neutrino oscillations in matter in the entire energy range.

To conclude, we have derived a simple closed-form analytic expression for the probability of two-flavour neutrino oscillations in a matter with an arbitrary density profile. Our formula is based on a perturbative expansion and allows an easy calculation of higher order corrections. We have applied our formalism to a number of density distributions, including the PREM density profile of the Earth, and demonstrated that the second-order approximation gives a very good accuracy in the entire energy interval.

Acknowledgments

We thank Andreas Hohenegger for the help with numerical calculations and Michele Maltoni for useful discussions.

References

- [1] L. Wolfenstein, Phys. Rev. **D17**, 2369 (1978).
- [2] S. P. Mikheev and A. Y. Smirnov, Sov. J. Nucl. Phys. **42**, 913 (1985).

- [3] P. C. de Holanda, W. Liao, and A. Y. Smirnov, Nucl. Phys. **B702**, 307 (2004), arXiv: [hep-ph/0404042](#) .
- [4] A. N. Ioannisian and A. Y. Smirnov, Phys. Rev. Lett. **93**, 241801 (2004), arXiv: [hep-ph/0404060](#) .
- [5] E. K. Akhmedov, M. A. Tortola, and J. W. F. Valle, JHEP **05**, 057 (2004), arXiv: [hep-ph/0404083](#) .
- [6] A. N. Ioannisian, N. A. Kazarian, A. Y. Smirnov, and D. Wyler, Phys. Rev. **D71**, 033006 (2005), arXiv: [hep-ph/0407138](#) .
- [7] E. K. Akhmedov, M. Maltoni, and A. Y. Smirnov, Phys. Rev. Lett. **95**, 211801 (2005), arXiv: [hep-ph/0506064](#) .
- [8] W. Liao, Phys. Rev. **D77**, 053002 (2008), arXiv: [0710.1492](#) .
- [9] A. D. Supanitsky, J. C. D’Olivo, and G. Medina-Tanco (2007), arXiv: [0708.0629](#) .
- [10] A. N. Ioannisian and A. Y. Smirnov (2008), arXiv: [0803.1967](#) .
- [11] A. M. Dziewonski and D. L. Anderson, Phys. Earth Planet. Interiors **25**, 297 (1981).
- [12] E. K. Akhmedov, Sov. J. Nucl. Phys. **47**, 301 (1988).
- [13] V. K. Ermilova, V. A. Tsarev, and V. A. Chechin, JETP Lett. **43**, 453 (1986).
- [14] D. Notzold, Phys. Rev. **D36**, 1625 (1987).
- [15] A. S. Dighe and A. Y. Smirnov, Phys. Rev. **D62**, 033007 (2000), arXiv: [hep-ph/9907423](#) .
- [16] E. K. Akhmedov, P. Huber, M. Lindner, and T. Ohlsson, Nucl. Phys. **B608**, 394 (2001), arXiv: [hep-ph/0105029](#) .
- [17] A. B. Balantekin, S. H. Fricke, and P. J. Hatchell, Phys. Rev. **D38**, 935 (1988).

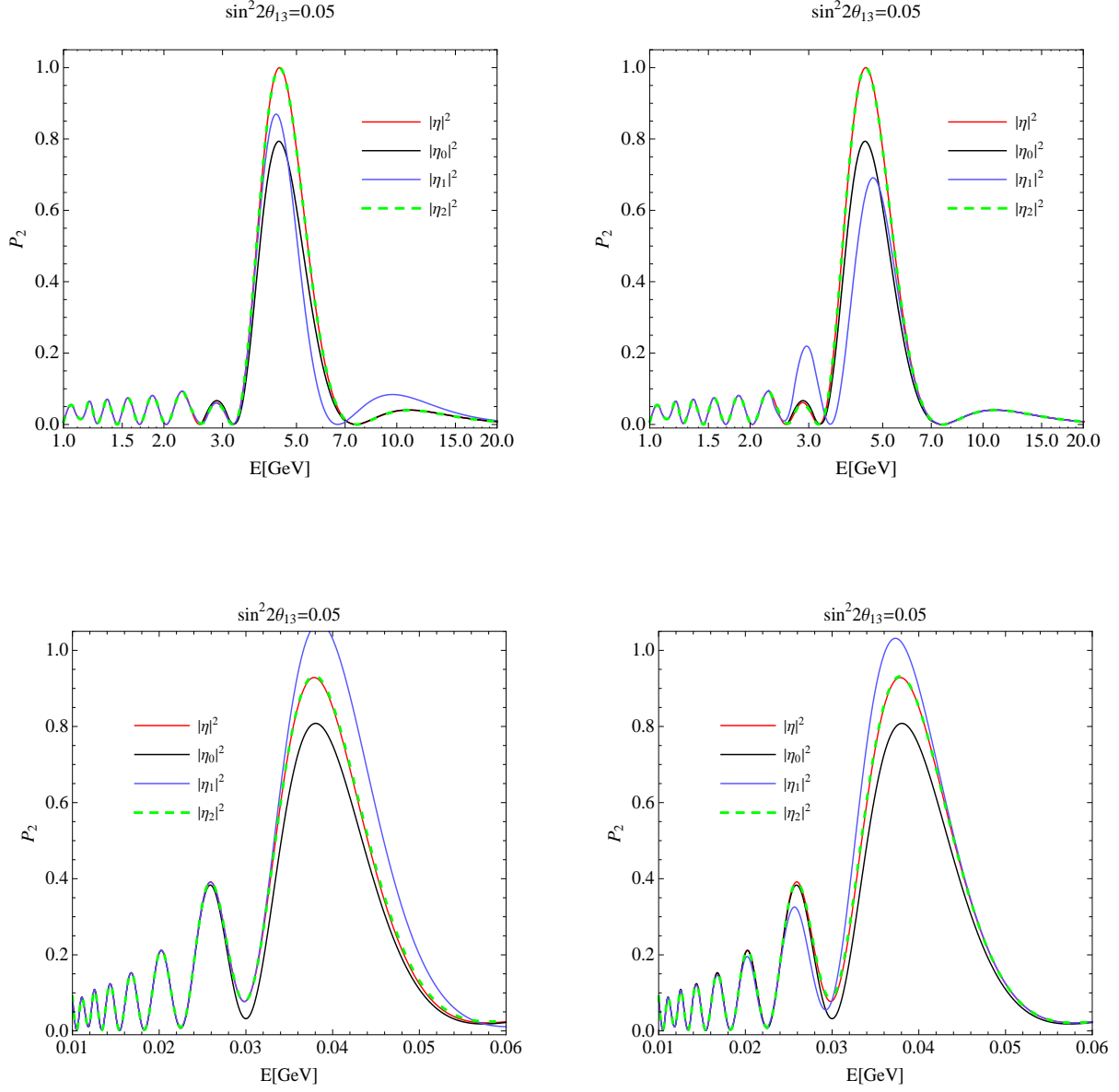


Figure 1: Oscillation probability P_2 versus neutrino energy E in the case of the parabolic (upper plots) and power law (lower plots) density profiles. Left panels: probabilities obtained from the expansion valid below the MSW resonance, right panels: the same for the expansion valid above the resonance. We have taken $\Delta m^2 = 2.5 \cdot 10^{-3} \text{ eV}^2$ and $Y_e = 0.5$.

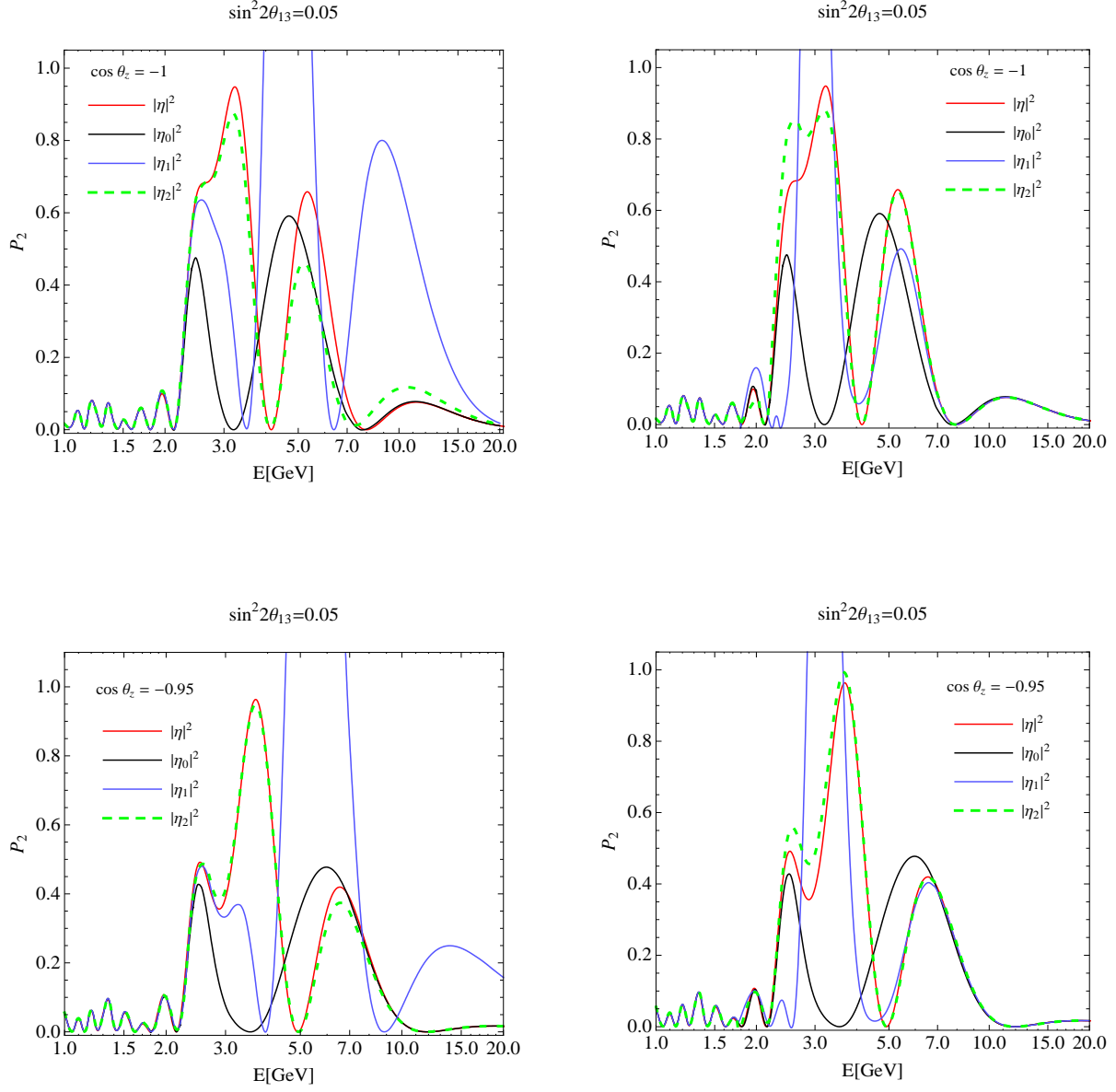


Figure 2: Probability P_2 versus neutrino energy E for neutrino oscillations in the Earth (PREM density profile) for two values of the zenith angle. Left panels: probabilities obtained from the expansion valid below the MSW resonance, right panels: the same for the expansion valid above the resonance. We have taken $\Delta m^2 = 2.5 \cdot 10^{-3} \text{ eV}^2$.

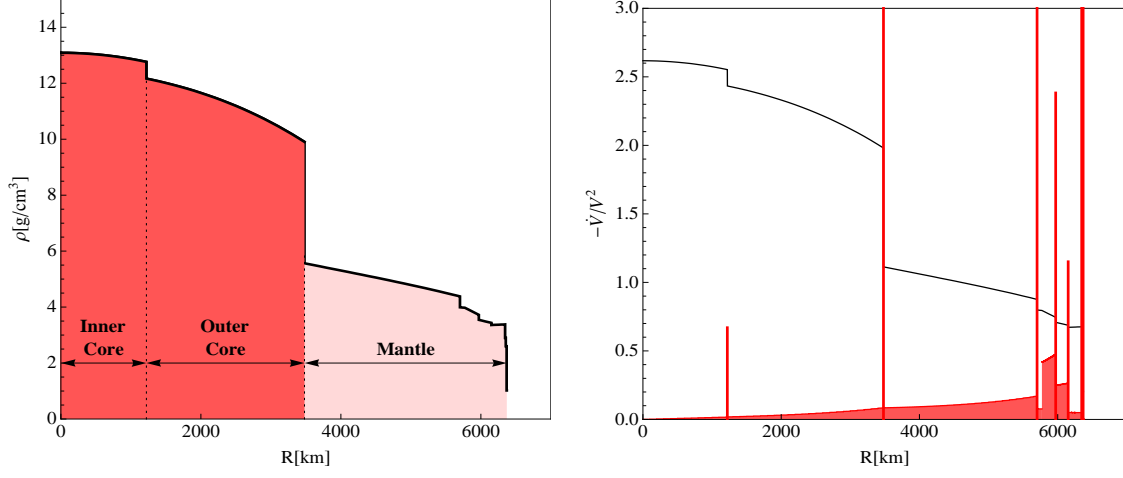


Figure 3: Left panel: matter density distribution inside the Earth as predicted by the PREM profile [11]. Right panel: the function $-\dot{V}/V^2$ as calculated with the PREM profile with density jumps smoothed over the distance of 30 km.

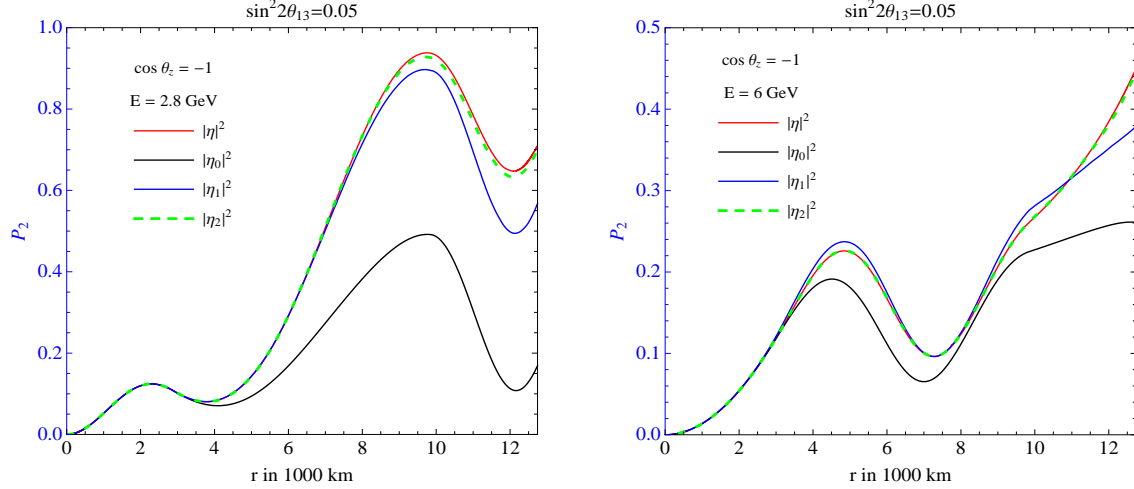


Figure 4: Oscillation probability P_2 in different orders in perturbation theory versus the distance travelled by neutrinos inside the Earth, for $\cos \theta_z = -1.0$ and for two values of neutrino energy ($E = 2.8$ GeV and 6 GeV). Left panels: probabilities obtained from the expansion valid below the MSW resonance, right panels: the same for the expansion valid above the resonance. We have taken $\Delta m^2 = 2.5 \cdot 10^{-3} \text{ eV}^2$.

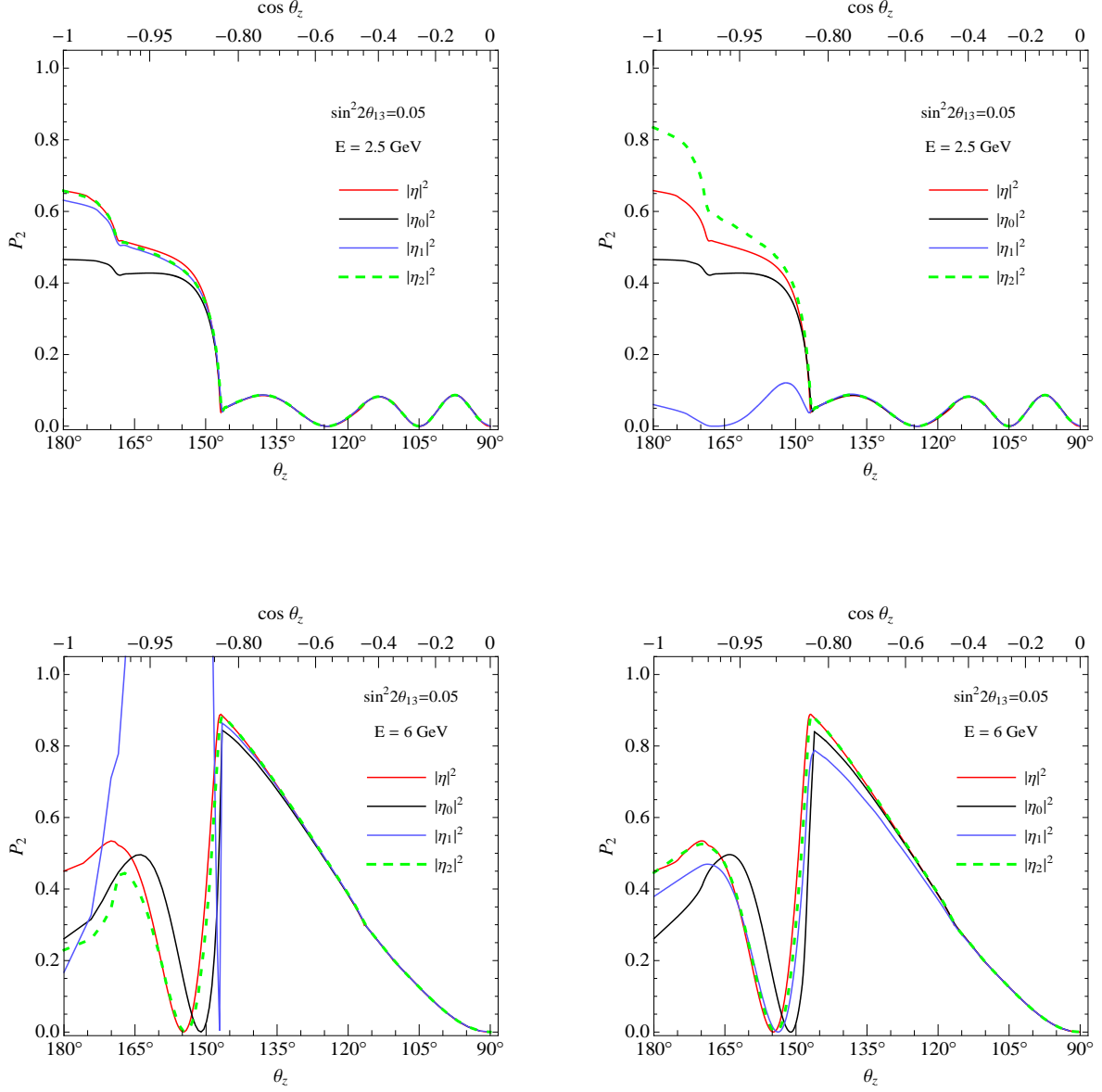


Figure 5: Oscillation probability P_2 versus the zenith angle θ_z for neutrinos propagating inside the Earth, for neutrino energies $E = 2.5$ and 6 GeV. Left panels: probabilities obtained from the expansion valid below the MSW resonance, right panels: the same for the expansion valid above the resonance. We have taken $\Delta m^2 = 2.5 \cdot 10^{-3} \text{ eV}^2$.

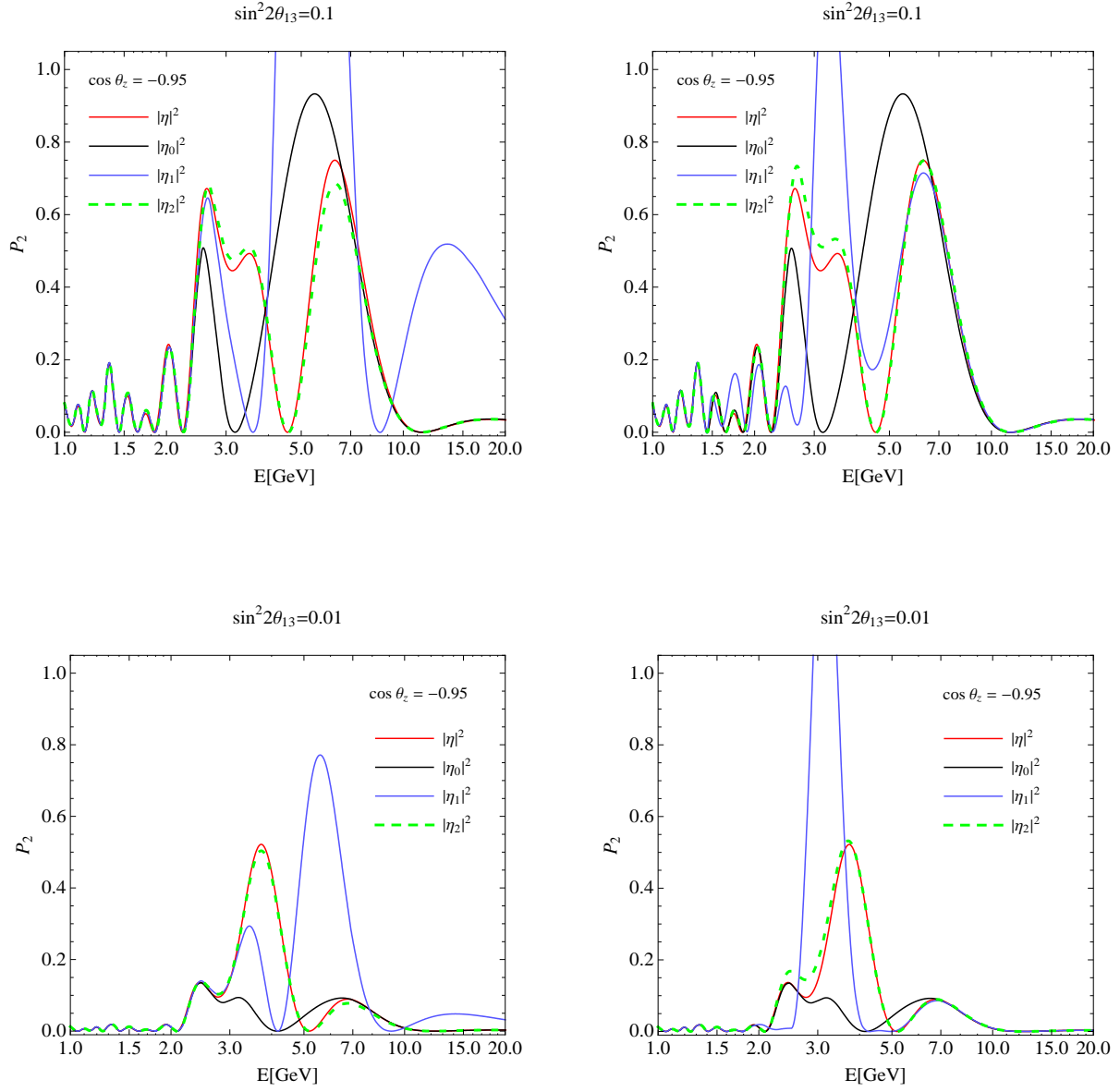


Figure 6: Oscillation probability P_2 versus neutrino energy E in the case of $\cos \theta_z = -0.95$ and for two different values of $\sin^2 2\theta_{13}$. Left panels: probabilities obtained from the expansion valid below the MSW resonance, right panels: the same for the expansion valid above the resonance. We have taken $\Delta m^2 = 2.5 \cdot 10^{-3} \text{ eV}^2$.